

# Paired associated magnetic stimulation promotes neural repair in the rat middle cerebral artery occlusion model of stroke

Bei-Yao Gao<sup>1,†</sup>, Cheng-Cheng Sun<sup>2,†</sup>, Guo-Hua Xia<sup>3</sup>, Shao-Ting Zhou<sup>4</sup>, Ye Zhang<sup>2</sup>, Ye-Ran Mao<sup>2</sup>, Pei-Le Liu<sup>1</sup>, Ya Zheng<sup>2</sup>, Dan Zhao<sup>2</sup>, Xu-Tong Li<sup>4</sup>, Janie Xu<sup>5</sup>, Dong-Sheng Xu<sup>2,\*</sup>, Yu-Long Bai<sup>1,\*</sup>

1 Department of Rehabilitation Medicine, Huashan Hospital, Fudan University, Shanghai, China

2 Rehabilitation Section, Department of Spine Surgery, Tongji Hospital, Medical School of Tongji University, Shanghai, China

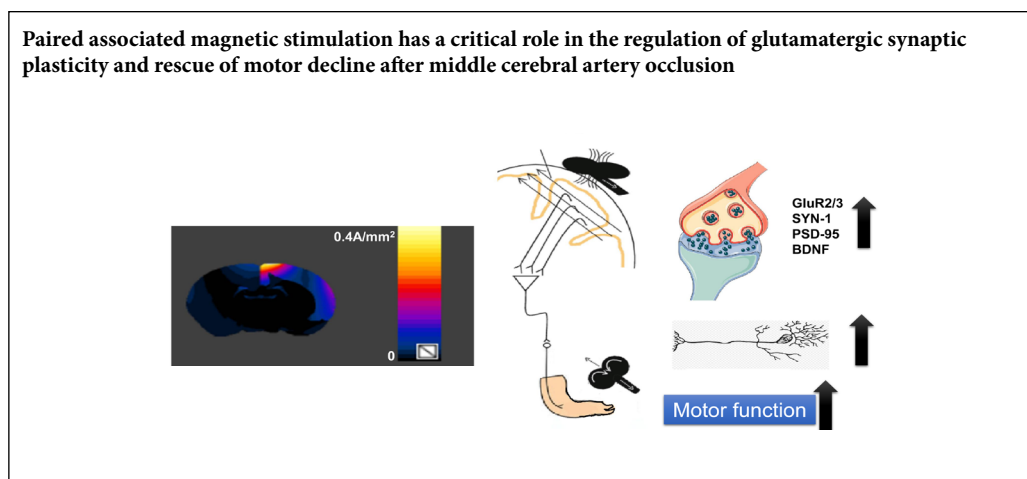
3 Department of Psychiatry and Behavioral Sciences, University of California, Davis, CA, USA

4 Department of Neurology, Minhang Hospital Affiliated to Fudan University, Shanghai, China

5 Brownell Talbot School, Omaha, NE, USA

**Funding:** This study was supported by the National Natural Science Foundation of China, Nos. 81974358, 81772453 (to DSX).

## Graphical Abstract



\*Correspondence to:

Dong-Sheng Xu, PhD,  
dxu0927@tongji.edu.cn;  
Yu-Long Bai, PhD,  
dr\_baiyl@fudan.edu.cn.

#Both authors contributed equally to this work.

orcid:

0000-0002-8477-5377  
(Dong-Sheng Xu)  
0000-0003-0461-1506  
(Yu-Long Bai)

doi: 10.4103/1673-5374.282266

Received: August 31, 2019

Peer review started: September 2, 2019

Accepted: November 7, 2019

Published online: May 11, 2020

## Abstract

Paired associative stimulation has been used in stroke patients as an innovative recovery treatment. However, the mechanisms underlying the therapeutic effectiveness of paired associative stimulation on neurological function remain unclear. In this study, rats were randomly divided into middle cerebral occlusion model (MCAO) and paired associated magnetic stimulation (PAMS) groups. The MCAO rat model was produced by middle cerebral artery embolization. The PAMS group received PAMS on days 3 to 20 post MCAO. The MCAO group received sham stimulation, three times every week. Within 18 days after ischemia, rats were subjected to behavioral experiments—the foot-fault test, the balance beam walking test, and the ladder walking test. Balance ability was improved on days 15 and 17, and the foot-fault rate was less in their affected limb on day 15 in the PAMS group compared with the MCAO group. Western blot assay showed that the expression levels of brain derived neurotrophic factor, glutamate receptor 2/3, postsynaptic density protein 95 and synapsin-1 were significantly increased in the PAMS group compared with the MCAO group in the ipsilateral sensorimotor cortex on day 21. Resting-state functional magnetic resonance imaging revealed that regional brain activities in the sensorimotor cortex were increased in the ipsilateral hemisphere, but decreased in the contralateral hemisphere on day 20. By finite element simulation, the electric field distribution showed a higher intensity, of approximately 0.4 A/m<sup>2</sup>, in the ischemic cortex compared with the contralateral cortex in the template. Together, our findings show that PAMS upregulates neuroplasticity-related proteins, increases regional brain activity, and promotes functional recovery in the affected sensorimotor cortex in the rat MCAO model. The experiments were approved by the Institutional Animal Care and Use Committee of Fudan University, China (approval No. 201802173S) on March 3, 2018.

**Key Words:** brain-derived neurotrophic factor; finite element simulation; glutamate receptor; ipsilateral hemisphere; paired associative stimulation; PSD95; resting-state functional MRI; stroke; synapsin I; transcranial magnetic stimulation

**Chinese Library Classification No.** R459.9; R363; R364

## Introduction

Stroke is a leading cause of death and severe disability in adults worldwide (Mozaffarian et al., 2016; Sarrafzadegan and Mohammadifard, 2019; Zhou et al., 2019). A non-in-

vasive method of cortical stimulation pairing transcranial magnetic stimulation (TMS) with a peripheral sensory stimulus, termed paired associative stimulation (PAS), has been shown to induce neuroplastic changes in the human motor,

somatosensory and auditory cortices (Tamura et al., 2009; Batsikadze et al., 2013). Peripheral muscle magnetic stimulation combined with repetitive transcranial magnetic stimulation has been used as a new therapeutic strategy in diseases such as chronic subjective tinnitus (Vielsmeier et al., 2018), but the underlying mechanisms remain unclear. PAS emphasizes the importance of somatosensory and intrinsic motor cortical circuits. Post-PAS excitability is considered a long-term potentiation-like phenomenon, and is associated with transient changes in synaptic efficacy in the glutamatergic system (Stefan et al., 2000, 2002). Conventional PAS targets the contralateral hemisphere.

In the current study, we investigate whether paired associated magnetic stimulation (PAMS) induces plastic changes in the brain on the affected and unaffected sides in the rat after stroke using brain imaging. We also examine whether magnetic stimulation effectively and specifically stimulates the ischemic affected brain tissue.

Neuroplasticity is the brain's ability to adapt to internal and external changes. In the early stage after stroke, because of neuronal death, functional connectivity between the ipsilesional and contralesional is impaired, resulting in functional loss. We previously evaluated the effect of the combination of electromagnetic stimulation and rehabilitation training based on the available evidence to establish a multimodal treatment strategy for nerve injury (Zheng et al., 2020). We also used modified constraint-induced movement therapy as a remodeling compensation model to study synaptic plasticity during stroke rehabilitation (Gao et al., 2020). Here, to better understand the neural plastic changes during the recovery stage, we use western blot assay to measure levels of plasticity-related proteins, including brain-derived neurotrophic factor (BDNF), AMAPR, synapsin I and PSD95 (as molecular biology indexes), and behavioral testing (as a functional index).

Blood oxygen level-dependent functional MRI (fMRI) is a method of assessing brain spatial functional changes induced by pharmacological therapy or rehabilitation. Plastic changes induced by PAMS are important for neural restoration, substitution and compensation after ischemic brain injury. In the present study, we assess neuroplasticity induced by middle cerebral artery occlusion (MCAO) using blood oxygen level-dependent functional magnetic resonance imaging (fMRI), with the amplitude of low-frequency fluctuation (ALFF) as a functional index.

Rat models are widely used in studies of various forms of magnetic stimulation. However, there is only limited knowledge on the distribution of the electric field induced by magnetic stimulation in the rat model of stroke, because computational models are lacking. In this study, we use computer simulation to locate the coil position by finite element analysis. The aim of computer simulation is to provide information on the effective range of PAMS and the magnetic field spatial distribution in the ipsilateral and contralateral hemispheres in MCAO rats. The innovative features of this study include the groundbreaking application of rodents in real and simulated situations, and the comprehensive study of neuro-

protection and neuroplasticity at the molecular and imaging levels in the ipsilateral and contralateral hemispheres.

In this study, we applied PAMS in the rat MCAO model, hypothesizing that PAMS activates the ipsilateral sensorimotor and sensory cortex, and that it upregulates the expression of brain plasticity-related proteins to ultimately change behavior. We also illustrate the electrical field distribution generated by magnetic stimulation in the rat template by finite element analysis.

## Materials and Methods

### Animals

Twelve male Sprague-Dawley rats, weighing 250–300 g and 7–9 weeks of age, were provided by Shanghai SIPPR-BK LAB Animal Ltd., China (license No. SCXK (Hu) 2013-0016). All rats were group-housed in clean but non-specific-pathogen-free animal facilities with free access to clean water and food under a 12/12-hour light/dark cycle. All experiments were approved by the Institutional Animal Care and Use Committee of Fudan University, China (approval No. 201802173S) on March 3, 2018. The experimental procedure followed the United States National Institutes of Health Guide for the Care and Use of Laboratory Animals (NIH Publication No. 85-23, revised 1996).

The rats were randomly divided into two groups ( $n = 6$ /group): MCAO group (only MCAO) and PAMS group (MCAO + PAMS).

### Production of the rat model of MCAO

Transient MCAO was performed as described previously (Liu et al., 2019). Briefly, the rat was anesthetized with 10% chloral hydrate (0.36 mL/100 g, intraperitoneally). A poly-L-lysine-coated filament (Beijing Cinontech Co., Ltd., Beijing, China) was inserted into the left middle cerebral artery for occlusion-induced ischemia. After a 90-minute period of ischemia, the filament was retracted. Blood flow was monitored by laser Doppler anemometry (Moor Instruments Ltd., Axminster, UK) immediately before and after ischemia. Then, 24 hours after surgery, neurologic deficits were assessed with neurological severity scores. Rats with scores of 1–3 were considered successful models, and others were excluded from the study.

### PAMS protocol

The PAMS protocol was based on clinical experience obtained from a pilot study of peripheral muscle magnetic stimulation as add-on treatment to repetitive TMS (rTMS) in rehabilitation medicine (Vielsmeier et al., 2018). The sensorimotor cortex was targeted and then marked by defining the motor threshold. Rats from the PAMS group underwent the following treatment procedure: 10 trials of repetitive peripheral magnetic stimulation and 2 trials of rTMS every three days from 3–20 days after MCAO. The TMS machine consisted of a Medtronic MagPro X100 stimulator (Medtronic, Copenhagen, Denmark). The diameter of the circular coil and the single diameter of the figure-8 coil were both 12 mm. Each treatment session consisted of three

phases: (1) repetitive peripheral magnetic stimulation of the elbow joint muscle group of the right upper limb and ankle joint muscle group of the right lower limb (20 Hz, 20 trains); (2) rTMS stimulation of the left (ipsilateral) sensorimotor cortex (60 Hz, 20 trains with an interval of 25 seconds); and (3) repetitive peripheral magnetic stimulation of the elbow joint muscle group of the right upper limb and ankle joint muscle group of the right lower limb (20 Hz, 20 trains). Phases 1 and 3 were done at a stimulation intensity of 30%, and phase 2 at 50%. The MCAO group was given sham stimulation, i.e., the same stimulation protocol, except that the coil was placed perpendicularly to the head. Motor-evoked potential was recorded in both groups before MCAO and on days 8, 14 and 20 after MCAO (Zhang et al., 2007; Luo et al., 2017; Caglayan et al., 2019). A concentric needle electrode was inserted in the gastrocnemius muscle of the right hind limb and connected to a Nicolet electromyographic device (Alpine Biomed, Skovlunde, Denmark); the ground wire was connected to the tail. Stimulator settings were as follows: time base 5 ms/div. and amplitude sensitivity 1 mV/div. Motor-evoked potential amplitudes (mV) in the left and right cortices were recorded separately.

#### Foot-fault test

The foot-fault test was used to assess placement dysfunction of the affected limb, as described previously (Liu et al., 2019). Briefly, each rat was required to pass the horizontal stepping test apparatus. The test was repeated three times in a blinded manner by the evaluator. The day of the MCAO was regarded as day 1. The test was performed on days 5, 7, 11, 15 and 18. If the limb missed or slipped on the rod, it was considered a wrong step. The ratio of the right front limb foot placement errors to the total number of steps was calculated by an analyzer who was blind to the experimental design.

#### Balance beam walking test

The rats walked the entire length of a standard balance beam (60 cm in length, 1.75 cm in width, 90 cm off the floor) steadily without falling off (Luong et al., 2011; Hausser et al., 2018). Briefly, a subjective observation was conducted for 60 seconds. Score 0 indicates stable balance; score 6 indicates fall off. The day of the MCAO was regarded as day 1. The test was performed in triplicate on days 5, 7, 11, 15, and 18. The average score of balance of each rat was calculated.

#### Ladder walking test

The ladder walking test was performed the same as foot-fault test. Analysis was made by inspection of the video recordings frame-by-frame as described in a previous study (Metz and Whishaw, 2009). Consecutive steps were analyzed. The last stepping cycle performed at the end of the ladder was excluded from scoring. Briefly, the seven scores of paw placement on the rungs were rated from total miss (0 point) to correct placement (6 points). The day of the MCAO was regarded as day 1. The test was performed on  $t =$  days 5, 7, 11, 15, 18. The average score of the right front limb step was calculated by an analyzer who was blind to the group information.

#### Western blot assay

The rats were killed on day 21 after MCAO. Brains were lysed in lysis buffer, and proteins were separated by sodium dodecyl sulfate-polyacrylamide gel electrophoresis (10%). All samples were transferred to a polyvinylidene fluoride membrane by wet transfer (Bio-Rad Laboratories AG, Frimburg, Switzerland). Membranes were incubated with primary antibodies—anti-PSD95, anti-glutamate receptor 2 & 3, anti-synapsin 1, anti-Bcl-2, anti-Bax, anti-PARP, anti- $\beta$ -tubulin or anti-GAPDH (Table 1) overnight at 4°C on a shaker. After three washes with Tris-buffered saline containing Tween 20, the membrane was incubated with the secondary antibody—horseradish peroxidase-conjugated Affinipure goat anti-mouse or horseradish peroxidase-conjugated Affinipure goat anti-rabbit (Table 1) for 60 minutes at room temperature. The protein bands were developed with an ECL detection kit (BeyoECL Moon, P0018FS, Beyotime Institute of Biotechnology, Haimen, China) and visualized with a DRAFT-FluorChem Q apparatus (Alpha Innotech Corporation, San Leandro, CA, USA). The optical densities of the bands were quantified with ImageJ 1.46a software (National Institutes of Health, Bethesda, MD, USA) and normalized to reference proteins (GAPDH and  $\beta$ -tubulin).

#### Enzyme-linked immunosorbent assay (ELISA)

The rats were killed on day 21 after MCAO. Sandwich Rat BDNF ELISA Kit (WESTANG BIO-TECH, Shanghai, China) involves the attachment of a capture antibody to a microplate. The samples were added and bound to the capture antibody anti-BDNF (Table 1). After washing, a horseradish peroxidase conjugate was added and detected with a DENLEY DRAGON WellsScan MK 3 (Thermo Fisher Scientific, Waltham, MA, USA). Multiskan Ascent software (Thermo Fisher Scientific) was used to draw a standard curve. The BDNF content was calculated according to the optical density value, and then multiplied by the dilution factor. All optical density values were calculated after subtracting the blank value.

#### MRI

Rats were anesthetized with isoflurane (1.5–2.5%) while monitoring respiration and controlling body temperature. MR scans were acquired on days 2 and 20 after MCAO on a MRI scanner (Bruker BioSpin, Rheinstetten, Germany) located at Fudan University Shanghai Cancer Center. For T2-weighted imaging, an initial RARE anatomical scan was acquired with a  $256 \times 256$  matrix, echo time = 33 ms, and 1-mm slice thickness. The scanning parameters were: slice thickness = 0.8000 mm, repetition time = 2500 ms, echo time = 33 ms, spacing between slices = 0.8000. For fMRI, echo-planar imaging parameters were as follows:  $90 \times 90$  matrix, repetition time = 3000 ms, echo time = 20 ms, 0.3000-mm slice thickness.

#### T2-weighted image analysis

T2 map image processing and format conversion were performed with MRI analysis software (ParaVision Acquisition 6.0). Researchers blinded to group identity measured the

**Table 1 Antibodies information**

Product name	Animal species	Description	Cat#	Concentration	Sources
Anti-PSD95	Mouse	Monoclonal	ab13552	1:500	Abcam, Cambridge CB2 0AX, UK
Anti-BDNF	Rabbit	Polyclonal	ab108319	1:1000	Abcam, Cambridge CB2 1AX, UK
Anti-glutamate receptor 2 & 3 Antibody	Rabbit	Polyclonal	ab1506	1:1000	Abcam, Cambridge CB2 2AX, UK
Anti-synapsin 1	Rabbit	Polyclonal	ab1543p	1:1000	Abcam, Cambridge CB2 3AX, UK
Anti-Bcl-2	Rabbit	Polyclonal	ab692	1:500	Abcam, Cambridge CB2 4AX, UK
Anti-Bax	Rabbit	Polyclonal	ab32503	1:1000	Abcam, Cambridge CB2 5AX, UK
Anti-PARP	Rabbit	Polyclonal	74290	1:1000	Abcam, Cambridge CB2 6AX, UK
Anti-β-tubulin	Mouse	Polyclonal	86298	1:5000	Cell Signaling Technology, Danvers, MA, USA
Anti-GAPDH	Mouse	Polyclonal	60004-1-Ig	1:5000	Proteintech, Wuhan, Hubei, China
HRP-conjugated Affinipure goat anti-mouse	Goat	Polyclonal	SA00001-1	1:1000	Proteintech, Wuhan, Hubei, China
HRP-conjugated Affinipure goat anti-rabbit	Goat	Polyclonal	SA00001-2	1:1000	Proteintech, Wuhan, Hubei, China

HRP: Horseradish peroxidase.

region of interest of each animal to quantify the ischemic volume. Relative infarct volume reduction was used to compare differences between the two groups. The infarct volume on day 2 after MCAO was subtracted from the infarct volume on day 20 to get the difference, and then divided by the infarct volume on day 2 (infarct volume reduction rate =  $\frac{\text{infarct volume}_{\text{day 20}} - \text{infarct volume}_{\text{day 2}}}{\text{infarct volume}_{\text{day 2}}}$ ).

### fMRI analysis

The magnetic resonance scan was performed on day 20 after MCAO using a 7.0 T Bruker Bio-Spin MR imaging system (Billerica, MA, USA). Anatomical features of the cerebellum and ventricles were used to position slices at the same location between sessions. Lesion volumes were measured with the MRI analysis software (ParaVision Acquisition 6.0) by an investigator blinded to group designation. SPM12 package (<https://www.fil.ion.ucl.ac.uk/spm/>) and MATLAB R2013 were used for functional data analysis. The functional images were preprocessed with origin re-determination, image amplification, and then by time slicing, realignment function, and co-registered to the subject's anatomical images in native space. The subject's deformation field maps obtained from the structural images were applied to the functional images to normalize them into the standard brain template. ALFF was calculated using the Resting-State fMRI Data Analysis Toolkit V1.7 (<http://www.restfmri.net>) in all subjects (Zou et al., 2009; Song et al., 2011). ALFF is the ratio of the power spectrum of 0.01–0.08 Hz to that of the entire frequency range, 0–0.25 Hz, for repetition time = 3 seconds. We performed ALFF calculations on the whole brain, and then compared the region of interest.

### Finite element mesh simulations

The experimental time began before the animal experiments because it is a computer-based simulation experiment. The three-dimensional (3D) brain model of Wistar rats was reconstructed using the public database from Tohoku University (<https://scalablebrainatlas.incf.org/>) and the open MRI

data from the Department of Psychiatry of the University of North Carolina at Chapel Hill. The blood supply region of the middle cerebral artery was labeled in original MRI data to build the MCAO rat brain 3D model using Sim4Life light software (ZMT, Zurich MedTech AG, Zurich, Switzerland), a simulation platform that can deal with MRI images. The figure-8 coil and circular coil parameters were referenced to model commercial coils (Wuhan Yiruide Medical Equipment New Technology Co., Ltd., Wuhan, China). A finite element method was used to solve the electromagnetic field distribution in the brain model (Capone et al., 2017; Samouidi et al., 2018). We set the permittivity and conductivity of the skull, dura mater, gray matter, white matter, cerebellum, spinal cord, cerebrospinal fluid and air at low frequencies separately. The electromagnetic field parameters, such as magnetic field strength H, magnetic flux density B, current density J, and electric displacement D distribution, were obtained through finite element analysis.

### Statistical analysis

All experimental data were analyzed using GraphPad Prism 7.0 software (GraphPad Software Inc., La Jolla, CA, USA) and SPSS 20.0 software (IBM Corporation, Armonk, NY, USA). The mean (average value) was reported along with a measure of variability standard deviation (s). Sample sizes were determined based on previous experience. No statistical methods were used to predetermine sample size. The foot-fault test score, balance beam walking test score, ladder walking test score, infarction volume, optical density of ELISA, and mean grey values for western blot assay were compared between the two groups by independent samples *t*-test. A value of  $P < 0.05$  was considered statistically significant. For fMRI statistical analysis, two samples *t*-tests were performed on ALFF maps by “Statistical Analysis” in REST, with cluster size > 10 voxels,  $P < 0.005$  (Zou et al., 2009; Yan and Zang, 2010; Song et al., 2011). A combined threshold of voxels of  $P < 0.001$  and cluster size > 35 mm<sup>3</sup> was considered significant, which corresponded with a corrected  $P < 0.05$ .

## Results

### PAMS improves neurobehavioral performance after MCAO

The experimental design is shown in **Figure 1A**. The overall PAMS treatment schedule is shown in **Figure 1B**. In the PAMS group, MEP waves on the ipsilateral and contralateral sides disappeared on day 8 after MCAO, and appeared again on day 14. MEP N1 wave and P1 wave were higher compared with before MCAO. The trend was still present on day 20, but with an even higher N1 on the contralateral side (**Figure 1C**). In the PAMS group, the TMS coil was positioned on the head (**Figure 1D**). Balance ability was improved in the PAMS group compared with the MCAO group on days 15 ( $P = 0.0049$ ) and 17 ( $P = 0.0006$ ) after ischemic brain injury. Foot-fault rate in the affected limb was lower in the PAMS group than in the MCAO group on day 15 after ischemic brain injury ( $P = 0.0317$ ). These results indicate that PAMS improves motor function (better balance and gait/grasp ability) after ischemic brain injury. No difference in walking ability of the affected upper limb was observed between the PAMS and MCAO groups within 18 days after ischemic brain injury (**Figure 2**).

### Safety of PAMS therapy after MCAO

The cerebral infarct volume was measured on day 2 and 20 after MCAO by MRI (**Figure 3**). Cerebral infarct volume in both groups was reduced on day 20 compared with day 2. However, the reduction in cerebral infarct volume was not significant in the two groups ( $P > 0.05$ ). These data demonstrate that PAMS may not help reduce infarct volume after ischemic brain injury. In addition, PARP, Bcl-2 and Bax expression levels were not significantly different between the PAMS and MCAO groups ( $P > 0.05$ ; **Figure 3**). Nonetheless, PAMS could be a safe and effective therapy for ischemic brain injury.

### Upregulation of GluR2/3, synapsin I, PSD95 and BDNF in the ipsilateral cortex in the PAMS group after MCAO

Western blot assay and ELISA were performed with tissue samples harvested from both ipsilateral and contralateral cortices of rats on day 21 after MCAO. PAMS strikingly increased GluR2/3, synapsin I, PSD95 and BDNF expression in the ipsilateral cortex ( $P < 0.05$ ; **Figure 4**). In comparison, the expression levels of GluR2/3, synapsin I, PSD95 and BDNF in the contralateral cortex were similar between the PAMS and MCAO groups.

### TMS treatment enhances the evoked fMRI signal in the ipsilateral hemisphere

There was a significant difference in ALFF between the MCAO and PAMS groups on day 20 after MCAO. In the contralateral cortex, an increased ALFF was detected in the MCAO group compared with the PAMS group. In contrast, in the ipsilateral sensory and sensorimotor cortices, ALFF was increased in the PAMS group compared with the MCAO group (**Figure 5**).

### Finite element analysis of magnetic stimulation-induced electrical field and magnetic field distribution in the 3D brain model of MCAO rats

The effects of different spatial positions of the figure-8 coil on the electromagnetic field distribution were studied (**Figure 6A and B**). The position in the deepest sensorimotor cortex was near anterior-posterior (AP) 3 mm, mediolateral (ML)  $\pm$  4 mm and dorsoventral (DV) 4 mm according to the brain map of the Wistar rat by Paxinos, George and Watson. The plane through this position (AP 3 mm; ML 4 mm; DV 4 mm) was used to select the position of the coil that would produce the strongest induced electric field. The figure-8 coil simulation results of the 3D MCAO rat model showed that, compared with the contralateral side, the distribution of the electromagnetic field within and around the liquefied necrotic area showed significantly enhanced current density (**Figure 6C**). The necrotic area increased around 4-fold, while the area around the necrosis increased more than 2-fold. The displacement current density in the necrotic area was close to zero, while the area around the necrosis was increased 2-fold. However, the magnetic field intensity and distribution were not different.

## Discussion

In the current study, we investigated the neuroprotective effect of PAMS, and found that it improved motor performance in rats with MCAO, and affected synaptic plasticity in the ipsilateral sensorimotor cortex. Moreover, resting-state fMRI showed that ALFF, as an index of regional neural activity, was increased in the sensorimotor cortex and sensory cortex in the ipsilateral motor hemisphere in the PAMS group compared with the MCAO group. A finite element method was used to solve the electromagnetic field distribution in the 3D standard and MCAO rat brain models. This showed that compared with the contralateral side, there is a greater distribution of the electromagnetic field within and around the liquefied necrotic area.

### PAMS safety and PAMS-induced plasticity

In this study, no difference was found in volume reduction or apoptosis-related protein expression after 3 weeks of PAMS treatment compared with the MCAO group. Thus, PAMS does not induce apoptosis, and appears safe. Furthermore, the recovery of neurological function probably involved brain plastic changes.

Many growth factors and other proteins are expressed in the intact brain region to help it to undergo plastic changes (Dahlqvist et al., 1999; Zhao et al., 2000, 2001). A primary mechanism in the control of synaptic strength during plasticity is a change in the number, composition and biophysical properties of AMPA-type glutamate receptors in the postsynaptic membrane (Diering and Huganir, 2018). Moreover, dysregulated AMPAR trafficking can lead to defects in the BDNF-tyrosine receptor kinase B signaling pathway by reducing the interaction between transmembrane AMPA receptor regulatory proteins and the PDZ-domain scaffold protein PSD95 (Zhang et al., 2018). These pathways

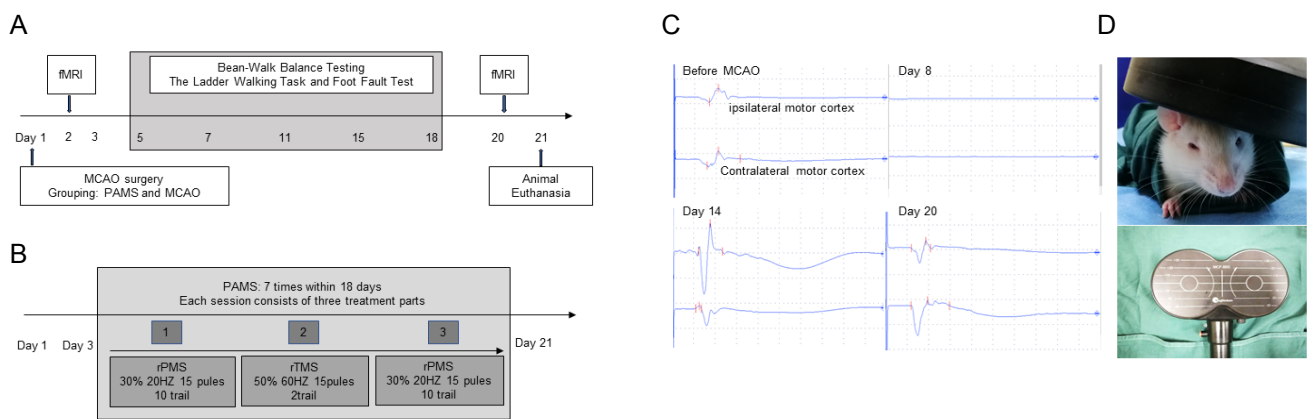


**Figure 1 Experimental design and PAMS.**

(A) Timeline of the MCAO PAMS experiments. (B) Overall treatment schedule of PAMS. (C) Motor-evoked potential in a rat from the PAMS group before and after MCAO. (D) Coil of the transcranial magnetic stimulation machine and simulation on a rat head. fMRI: Functional magnetic resonance imaging; MCAO: middle cerebral artery occlusion; PAMS: paired associated magnetic stimulation; rPMS: repetitive peripheral magnetic stimulation; rTMS: repetitive transcranial magnetic stimulation.

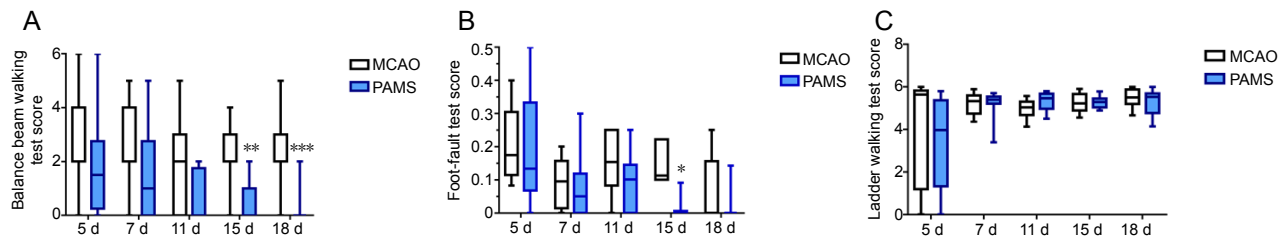


**Figure 2 Effects of PAMS on balance and motor functions after MCAO.**

(A) Balance beam walking test. Balance ability was improved in the PAMS group compared with the MCAO group on days 15 and 17 after ischemic brain injury. (B) Foot-fault test. Foot-fault rate in the affected limb was lower in the PAMS group than in the MCAO group on day 15 after ischemic brain injury. (C) Ladder walking test. No difference in the affected upper limb was found between the PAMS and MCAO groups within 18 days after ischemic brain injury. Data are expressed as the mean  $\pm$  SD ( $n = 6$ ; independent samples  $t$ -test). \* $P < 0.05$ , \*\* $P < 0.01$ , \*\*\* $P < 0.001$ , vs. MCAO group. MCAO: Middle cerebral artery occlusion; PAMS: paired associated magnetic stimulation.

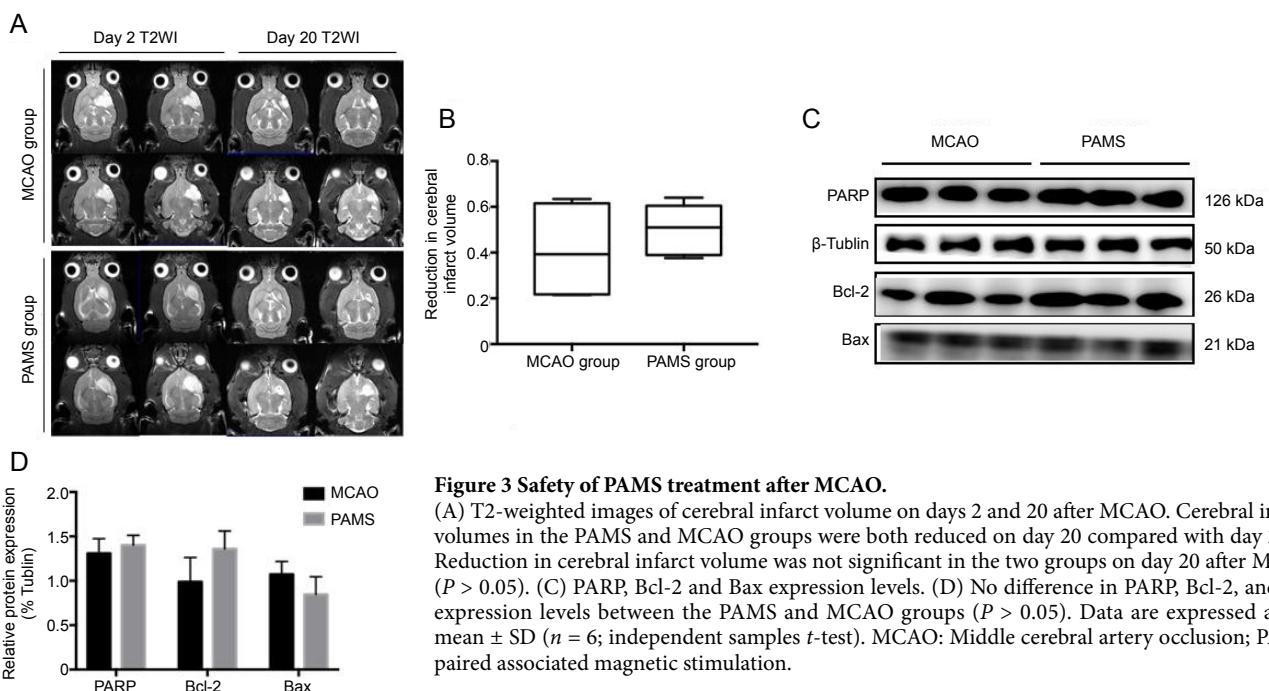


**Figure 3 Safety of PAMS treatment after MCAO.**

(A) T2-weighted images of cerebral infarct volume on days 2 and 20 after MCAO. Cerebral infarct volumes in the PAMS and MCAO groups were both reduced on day 20 compared with day 2. (B) Reduction in cerebral infarct volume was not significant in the two groups on day 20 after MCAO ( $P > 0.05$ ). (C) PARP, Bcl-2 and Bax expression levels. (D) No difference in PARP, Bcl-2, and Bax expression levels between the PAMS and MCAO groups ( $P > 0.05$ ). Data are expressed as the mean  $\pm$  SD ( $n = 6$ ; independent samples  $t$ -test). MCAO: Middle cerebral artery occlusion; PAMS: paired associated magnetic stimulation.

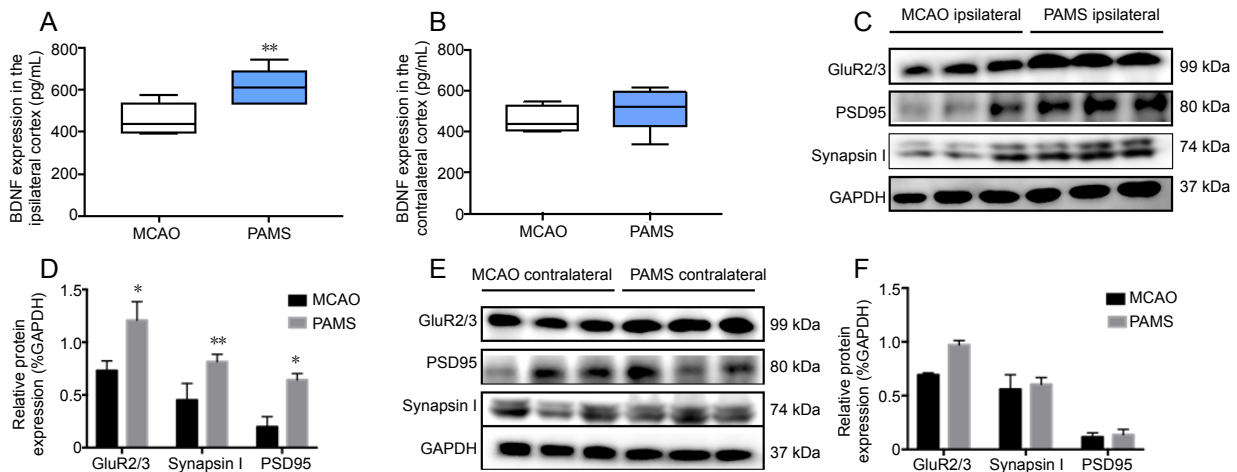


**Figure 4 Upregulation of GluR2/3, synapsin I, PSD95 and BDNF in the ipsilateral sensorimotor cortex in the PAMS group on day 21 after MCAO.** (A) ELISA of BDNF expression in the ipsilateral and contralateral sensorimotor cortices. PAMS robustly increased BDNF expression in the ipsilateral sensorimotor cortex on day 21 after MCAO. (B) There was no difference in BDNF content between the MCAO and PAMS groups in the contralateral sensorimotor cortex. (C) Western blot assay of tissue samples harvested from ipsilateral cortex of rats on day 21 after MCAO. (D) PAMS strongly increased GAPDH-normalized protein levels of GluR2/3, synapsin I and PSD95 in the ipsilateral cortex compared with the MCAO group. (E) Western blot assay of tissue samples harvested from the contralateral cortex of rats on day 21 after MCAO. (F) Graphs show GAPDH-normalized protein levels of GluR2/3, synapsin I and PSD95 in the contralateral cortex. Data are expressed as the mean  $\pm$  SD ( $n = 6$ ; independent samples  $t$ -test). \* $P < 0.05$ , \*\* $P < 0.01$ , vs. MCAO group. BDNF: Brain-derived neurotrophic factor; MCAO: middle cerebral artery occlusion; PAMS: paired associated magnetic stimulation.

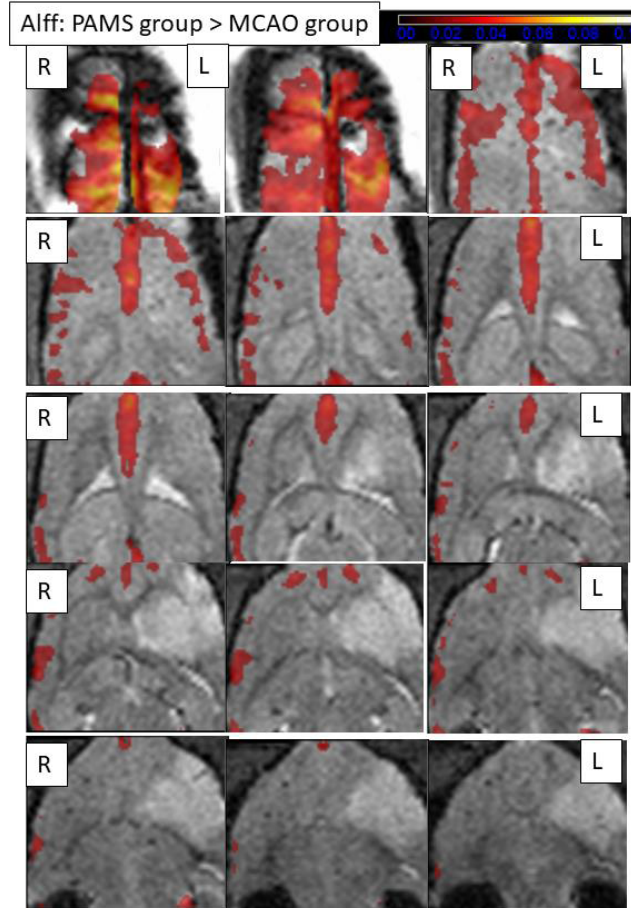


**Figure 5 Comparisons of the amplitude of low-frequency fluctuations (ALFF) between the two groups 20 days after MCAO (fMRI).** Resting-state fMRI of ALFF 20 days after MCAO. ALFF maps showing the PAMS group subtracted from the MCAO group (cluster size  $> 10$  voxels; two samples  $t$ -test,  $P < 0.005$ ). A larger ALFF signal difference is detected in the cortex around the ischemic periphery in the bilateral cortex compared with the MCAO group. The color bars indicate the  $t$ -value of the group analysis (the brighter the color, the higher the value) (fMRI). L: Ipsilateral cortex; R: contralateral cortex.

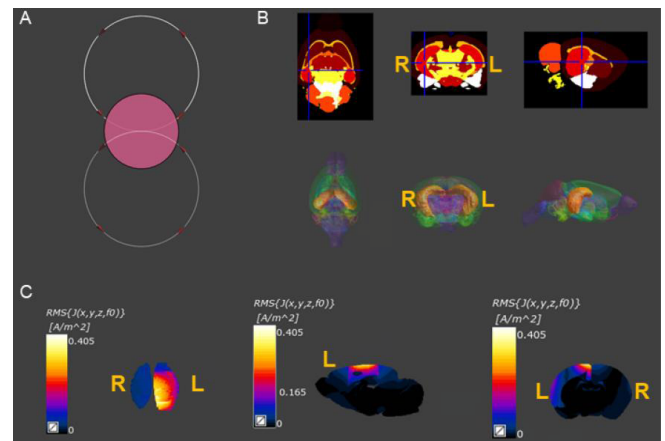


**Figure 6 Finite element analysis of the magnetic stimulation-induced electrical field and magnetic field distribution in the 3D brain model of MCAO rats.** (A) Effects of different spatial positions of the figure-8 coil on the electromagnetic field distribution: The diameter of the circular coil and the single diameter of the figure-8 coil were both 12 mm. The coils were placed 2 mm above the plane of the head. (B) The 3D model included 154 brain regions, and the corresponding conductivity and permittivity according to the physical properties of the brain tissues. (C) The figure-8 coil simulation results of the 3D model of MCAO rats. Compared with the contralateral side, the distribution of the electromagnetic field within and around the liquefied necrotic area showed significantly enhanced current density. 3D: Three-dimensional; L: ipsilateral cortex; R: contralateral cortex.

play a key role in activity-dependent treatments, including electrical stimulation, exercise and magnetic stimulation (Cheeran et al., 2008; Player et al., 2013; McGregor and English, 2018). In addition, BDNF-mediated synaptic and neurodevelopmental processes require functional integrity of membrane lipid rafts, which is maintained by synapsins (Kao et al., 2017). Synapsin I is an important modulator of synaptic plasticity in both the ipsilateral and contralateral

brain regions after ischemic injury (Shih et al., 2013; Pan et al., 2017), and participates in the enhancement of synaptic vesicle recycling (Kohl et al., 2019). These proteins are closely related to plasticity. Our current results show that these proteins are affected by PAMS treatment.

### Finite element analysis of simulated electromagnetic field distribution

Here, we investigated the electromagnetic field distribution in the brain of MCAO rats given TMS to identify effective stimulation sites and parameters. Finite element analysis was used to simulate the physical phenomenon (PAMS) using the numerical algorithm technique so as to reduce the number of physical prototypes and experiments and optimize components in our design phase to develop better methodology. Most TMS studies have been performed in humans, and research on animal stroke models is still lacking. The TMS parameters currently applied to MCAO rats are based on clinical parameters. The most commonly used frequency parameters are 20, 10, 5, 1, 0.5 and 0.05 Hz (Zhang et al., 2007; Gao et al., 2010; Li et al., 2012; Beom et al., 2015; Caglayan et al., 2019). In the present study, we applied 60 Hz stimulation, and finite element analysis showed that this stimulation method could distribute the electric field in the affected brain region. There is evidence to support our approach. For example, TMS in theta frequency (relatively high frequency greater than 50 Hz) bursts may produce lasting neuroplastic changes in the human cortex, and may be a safe and effective treatment for major depressive disorder (Blumberger et al., 2018). In the present study, we directly stimulated the ipsilateral brain with TMS, not the contralateral brain. In the simulation, the position at which the coil was placed was determined by the maximum current sensed in the affected brain under the same magnetic stimulation parameters, calculated by finite element analysis. Our finite element analysis could be used to optimize TMS coil parameters and provide a basis for future TMS studies on MCAO animal models. Our findings also provide a theoretical foundation for accurate TMS positioning in animal experiments and for the use of high-frequency parameter settings.

In the present study, we modified the PAS protocol, and proposed the PAMS protocol, which combines magnetic stimulation of the affected limb muscle and high-frequency transcranial magnetic stimulation of the ipsilesional sensorimotor cortex, and tested whether it helps improve ipsilesional neural circuit reorganization and neurological function after ischemic brain injury. We have innovatively used rodent models in real and simulated situations, and we have comprehensively studied all aspects of neuroprotection and neuroplasticity at the different molecular and imaging levels in the ipsilateral and contralateral hemispheres.

There are some limitations to our study. For example, because PAMS is a combination of two non-invasive neurorehabilitative technologies, the animal subjects should have been further divided into subgroups for a more comprehensive assessment. It is also challenging to link PAMS-induced changes in brain activity with changes in synaptic plasticity-

ty-related proteins by fMRI, owing to the lack of technical information. Furthermore, because our simulation did not involve information about the skull, it was not fully consistent with the actual situation. Further improvements are needed in future studies.

### Conclusions

In this study, we investigated the effect of PAMS on the ipsilateral and contralateral sensorimotor cortices in the rat MCAO model of stroke. PAMS treatment for 3 weeks improved motor behavior in MCAO rats, and it did not up-regulate apoptosis-related proteins. Moreover, the synaptic plasticity-associated proteins synapsin I, PSD95, GluR2/3 and BDNF were upregulated in the ipsilateral sensorimotor cortex, but not in the contralateral cortex. In addition, ALFF was increased in the ipsilateral motor and sensory cortices in the PAMS group compared with the MCAO group. We generated a 3D brain template by MRI and illustrated the distribution of the electromagnetic field with coil positioning by finite element analysis. Collectively, our findings suggest that PAMS promotes neural repair by activating the ipsilateral sensorimotor cortex and by stimulating synaptic plasticity. Further studies should focus not only on PAMS but also on magnetic stimulation of other neural circuits.

**Acknowledgments:** The authors thank for Professor Min Zhao and Professor Wei-Jian Yang from University of California, Davis for their help with finite element analysis.

**Author contributions:** Study design: YLB, BYG, and DSX; in vitro experiments: CCS, STZ, and XTL; in vivo experiments: BYG, YaZ, PLL, DZ, and YeZ; EMG performance: GHX, YRM, and JX; manuscript writing: BYG; experimental supervision, statistical analysis and manuscript revision: YLB, and DSX. All authors read and approved the final manuscript.

**Conflicts of interest:** All authors claim no financial and personal relationships with other people or organizations that could inappropriately influence (bias) their work.

**Financial support:** This study was supported by the National Natural Science Foundation of China, Nos. 81974358, 81772453 (to DSX).

**Institutional review board statement:** All experiments were approved by the Institutional Animal Care and Use Committee of Fudan University, China (approval No. 201802173S) on March 3, 2018. The experimental procedure followed the United States National Institutes of Health Guide for the Care and Use of Laboratory Animals (NIH Publication No. 85-23, revised 1996).

**Copyright license agreement:** The Copyright License Agreement has been signed by all authors before publication.

**Data sharing statement:** Datasets analyzed during the current study are available from the corresponding author on reasonable request.

**Plagiarism check:** Checked twice by iThenticate.

**Peer review:** Externally peer reviewed.

**Open access statement:** This is an open access journal, and articles are distributed under the terms of the Creative Commons Attribution-Non-Commercial-ShareAlike 4.0 License, which allows others to remix, tweak, and build upon the work non-commercially, as long as appropriate credit is given and the new creations are licensed under the identical terms.

### References

- Batsikadze G, Paulus W, Kuo MF, Nitsche MA (2013) Effect of serotonin on paired associative stimulation-induced plasticity in the human sensorimotor cortex. *Neuropsychopharmacology* 38:2260-2267.
- Beom J, Kim W, Han TR, Seo K, Oh B (2015) Concurrent use of granulocyte-colony stimulating factor with repetitive transcranial magnetic stimulation did not enhance recovery of function in the early subacute stroke in rats. *Neurol Sci* 36:771-777.

- Blumberger DM, Vila-Rodriguez F, Thorpe KE, Feffer K, Noda Y, Giacobbe P, Knyahnytska Y, Kennedy SH, Lam RW, Daskalakis ZJ, Downar J (2018) Effectiveness of theta burst versus high-frequency repetitive transcranial magnetic stimulation in patients with depression (THREE-D): a randomised non-inferiority trial. *Lancet* 391:1683-1692.
- Caglayan AB, Beker MC, Caglayan B, Yalcin E, Caglayan A, Yulug B, Hanoglu L, Kutlu S, Doeppner TR, Hermann DM, Kilic E (2019) Acute and post-acute neuromodulation induces stroke recovery by promoting survival signaling, neurogenesis, and pyramidal tract plasticity. *Front Cell Neurosci* 13: 144.
- Capone F, Liberti M, Apollonio F, Camera F, Setti S, Cadossi R, Quattrocchi CC, Di Lazzaro V (2017) An open-label, one-arm, dose-escalation study to evaluate safety and tolerability of extremely low frequency magnetic fields in acute ischemic stroke. *Sci Rep* 7:12145.
- Caras ML, Sanes DH (2017) Top-down modulation of sensory cortex gates perceptual learning. *Proc Natl Acad Sci U S A* 114:9972-9977.
- Chao-Gan Y, Yu-Feng Z (2010) DPARSF: A MATLAB toolbox for "Pipeline" data analysis of resting-state fMRI. *Front Syst Neurosci* 4:13.
- Cheeran B, Talelli P, Mori F, Koch G, Suppa A, Edwards M, Houlden H, Bhatia K, Greenwood R, Rothwell JC (2008) A common polymorphism in the brain-derived neurotrophic factor gene (BDNF) modulates human cortical plasticity and the response to rTMS. *J Physiol* 586:5717-5725.
- Cunningham DA, Varnerin N, Machado A, Bonnett C, Janini D, Roelle S, Potter-Baker K, Sankarasubramanian V, Wang X, Yue G, Plow EB (2015) Stimulation targeting higher motor areas in stroke rehabilitation: A proof-of-concept, randomized, double-blinded placebo-controlled study of effectiveness and underlying mechanisms. *Restor Neurol Neurosci* 33:911-926.
- Dahlqvist P, Zhao L, Johansson IM, Mattsson B, Johansson BB, Seckl JR, Olsson T (1999) Environmental enrichment alters nerve growth factor-induced gene A and glucocorticoid receptor messenger RNA expression after middle cerebral artery occlusion in rats. *Neuroscience* 93:527-535.
- Di Lazzaro V, Capone F, Di Pino G, Pellegrino G, Florio L, Zollo L, Simonetti D, Ranieri F, Brunelli N, Corbetto M, Miccinilli S, Bravi M, Milighetti S, Guglielmelli E, Sterzi S (2016) Combining robotic training and non-invasive brain stimulation in severe upper limb-impaired chronic stroke patients. *Front Neurosci* 10:88.
- Diering GH, Haganir RL (2018) The AMPA receptor code of synaptic plasticity. *Neuron* 100:314-329.
- Feng HL, Yan L, Cui LY (2008) Effects of repetitive transcranial magnetic stimulation on adenosine triphosphate content and microtubule associated protein-2 expression after cerebral ischemia-reperfusion injury in rat brain. *Chin Med J (Engl)* 121:1307-1312.
- Fleming MK, Sorinola IO, Roberts-Lewis SF, Wolfe CD, Wellwood I, Newham DJ (2015) The effect of combined somatosensory stimulation and task-specific training on upper limb function in chronic stroke: a double-blind randomized controlled trial. *Neurorehabil Neural Repair* 29:143-152.
- Gao BY, Xu DS, Liu PL, Li C, Du L, Hua Y, Hu J, Hou JY, Bai YL (2020) Modified constraint-induced movement therapy alters synaptic plasticity of rat contralateral hippocampus following middle cerebral artery occlusion. *Neural Regen Res* 15:1045-1057.
- Gao F, Wang S, Guo Y, Wang J, Lou M, Wu J, Ding M, Tian M, Zhang H (2010) Protective effects of repetitive transcranial magnetic stimulation in a rat model of transient cerebral ischaemia: a microPET study. *Eur J Nucl Med Mol Imaging* 37:954-961.
- Gehwolf R, Schwemberger B, Jessen M, Korntner S, Wagner A, Lehner C, Weissenbacher N, Tempfer H, Traweger A (2019) Global responses of IL-1 $\beta$ -Primed 3D tendon constructs to treatment with pulsed electromagnetic fields. *Cells* 8:399.
- Guo F, Lou J, Han X, Deng Y, Huang X (2017) Repetitive transcranial magnetic stimulation ameliorates cognitive impairment by enhancing neurogenesis and suppressing apoptosis in the hippocampus in rats with ischemic stroke. *Front Physiol* 8:559.
- Hausser N, Johnson K, Parsley MA, Guptarak J, Spratt H, Sell SL (2018) Detecting behavioral deficits in rats after traumatic brain injury. *J Vis Exp* doi:10.3791/56044.
- Kao HT, Ryoo K, Lin A, Janoschka SR, Augustine GJ, Porton B (2017) Synapsins regulate brain-derived neurotrophic factor-mediated synaptic potentiation and axon elongation by acting on membrane rafts. *Eur J Neurosci* 45:1085-1101.
- Kohl S, Hannah R, Rocchi L, Nord CL, Rothwell J, Voon V (2019) Cortical paired associative stimulation influences response inhibition: cortico-cortical and cortico-subcortical networks. *Biol Psychiatry* 85:355-363.
- Kozel FA, Motes MA, Didehbani N, DeLaRosa B, Bass C, Schraufnagel CD, Jones P, Morgan CR, Spence JS, Kraut MA, Hart JJ (2018) Repetitive TMS to augment cognitive processing therapy in combat veterans of recent conflicts with PTSD: a randomized clinical trial. *J Affect Disord* 229:506-514.
- Laura G, Silvia T, Nikolaos P, Patrizia P (2018) The role of fMRI in the assessment of neuroplasticity in MS: a systematic review. *Neural Plast* 2018:3419871.
- Li M, Peng J, Song Y, Liang H, Mei Y, Fang Y (2012) Electro-acupuncture combined with transcranial magnetic stimulation improves learning and memory function of rats with cerebral infarction by inhibiting neuron cell apoptosis. *Huazhong Keji Daxue Xuebao* 32:746-749.
- Lin YN, Hu CJ, Chi JY, Lin LF, Yen TH, Lin YK, Liou TH (2015) Effects of repetitive transcranial magnetic stimulation of the unaffected hemisphere leg motor area in patients with subacute stroke and substantial leg impairment: a pilot study. *J Rehabil Med* 47:305-310.
- Liu P, Li C, Zhang B, Zhang Z, Gao B, Liu Y, Wang Y, Hua Y, Hu J, Qiu X, Bai Y (2019) Constraint induced movement therapy promotes contralesional-oriented structural and bihemispheric functional neuroplasticity after stroke. *Brain Res Bull* 150:201-206.
- Luo J, Zheng H, Zhang L, Zhang Q, Li L, Pei Z, Hu X (2017) High-frequency repetitive transcranial magnetic stimulation (rTMS) improves functional recovery by enhancing neurogenesis and activating BDNF/TrkB signaling in ischemic rats. *Int J Mol Sci* 18:455.
- Luong TN, Carlisle HJ, Southwell A, Patterson PH (2011) Assessment of motor balance and coordination in mice using the balance beam. *J Vis Exp* doi:10.3791/2376
- McGann JP (2015) Associative learning and sensory neuroplasticity: how does it happen and what is it good for? *Learn Mem* 22:567-576.
- McGregor CE, English AW (2018) The role of BDNF in peripheral nerve regeneration: activity-dependent treatments and Val66Met. *Front Cell Neurosci* 12:522.
- Metz GA, Whishaw IQ (2009) The ladder rung walking task: a scoring system and its practical application. *J Vis Exp* doi:10.3791/1204.
- Mozaffarian D, Benjamin EJ, Go AS, Arnett DK, Blaha MJ, Cushman M, Das SR, de Ferranti S, Després JP, Fullerton HJ, Howard VJ, Huffman MD, Iqbal S, Jimenez MC, Judd SE, Kissela BM, Lichtman JH, Lisabeth LD, Liu S, Mackey RH, et al. (2016) Heart disease and stroke statistics-2016 update: a report from the American Heart Association. *Circulation* 133:e38-360.

- Ohlsson AL, Johansson BB (1995) Environment influences functional outcome of cerebral infarction in rats. *Stroke* 26:644-649.
- Pan R, Cai J, Zhan L, Guo Y, Huang RY, Li X, Zhou M, Xu D, Zhan J, Chen H (2017) Buyang Huanwu decoction facilitates neurorehabilitation through an improvement of synaptic plasticity in cerebral ischemic rats. *BMC Complement Altern Med* 17:173.
- Player MJ, Taylor JL, Weickert CS, Alonzo A, Sachdev P, Martin D, Mitchell PB, Loo CK (2013) Neuroplasticity in depressed individuals compared with healthy controls. *Neuropsychopharmacology* 38:2101-2108.
- Samoudi AM, Tanghe E, Martens L, Joseph W (2018) Deep transcranial magnetic stimulation: improved coil design and assessment of the induced fields using mda model. *Biomed Res Int* 2018:7061420.
- Sarrafzadegan N, Mohammadifard N (2019) Cardiovascular disease in Iran in the last 40 years: prevalence, mortality, morbidity, challenges and strategies for cardiovascular prevention. *Arch Iran Med* 22:204-210.
- Sathappan AV, Lubner BM, Lisanby SH (2019) The dynamic duo: combining noninvasive brain stimulation with cognitive interventions. *Prog Neuropsychopharmacol Biol Psychiatry* 89:347-360.
- Schenk U, Menna E, Kim T, Passafaro M, Chang S, De Camilli P, Matteoli M (2005) A novel pathway for presynaptic mitogen-activated kinase activation via AMPA receptors. *J Neurosci* 25:1654-1663.
- Shih PC, Yang YR, Wang RY (2013) Effects of exercise intensity on spatial memory performance and hippocampal synaptic plasticity in transient brain ischemic rats. *PLoS One* 8:e78163.
- Song XW, Dong ZY, Long XY, Li SF, Zuo XN, Zhu CZ, He Y, Yan CG, Zang YF (2011) REST: a toolkit for resting-state functional magnetic resonance imaging data processing. *PLoS One* 6:e25031.
- Stefan K, Kunesch E, Cohen LG, Benecke R, Classen J (2000) Induction of plasticity in the human sensorimotor cortex by paired associative stimulation. *Brain* 123:572-584.
- Stefan K, Kunesch E, Benecke R, Cohen LG, Classen J (2002) Mechanisms of enhancement of human sensorimotor cortex excitability induced by interventional paired associative stimulation. *J Physiol* 543:699-708.
- Tamura Y, Ueki Y, Lin P, Vorbach S, Mima T, Kakigi R, Hallett M (2009) Disordered plasticity in the primary somatosensory cortex in focal hand dystonia. *Brain* 132:749-755.
- Tsagaris KZ, Labar DR, Edwards DJ (2016) A framework for combining rTMS with behavioral therapy. *Front Syst Neurosci* 10:82.
- Vielsmeier V, Schecklmann M, Schlee W, Kreuzer PM, Poeppel TB, Rupprecht R, Langguth B, Lehner A (2018) A pilot study of peripheral muscle magnetic stimulation as add-on treatment to repetitive transcranial magnetic stimulation in chronic tinnitus. *Front Neurosci* 12:68.
- Wang RY, Wang FY, Huang SF, Yang YR (2019) High-frequency repetitive transcranial magnetic stimulation enhanced treadmill training effects on gait performance in individuals with chronic stroke: a double-blinded randomized controlled pilot trial. *Gait Posture* 68:382-387.
- Yuan R, Di X, Kim EH, Barik S, Rypma B, Biswal BB (2013) Regional homogeneity of resting-state fMRI contributes to both neurovascular and task activation variations. *Magn Reson Imaging* 31:1492-1500.
- Zhang H, Zhang C, Vincent J, Zala D, Benstaali C, Sainlos M, Grillo-Bosch D, Daburon S, Coussen F, Cho Y, David DJ, Saudou F, Humeau Y, Choquet D (2018) Modulation of AMPA receptor surface diffusion restores hippocampal plasticity and memory in Huntington's disease models. *Nat Commun* 9:4272.
- Zhang X, Mei Y, Liu C, Yu S (2007) Effect of transcranial magnetic stimulation on the expression of c-Fos and brain-derived neurotrophic factor of the cerebral cortex in rats with cerebral infarct. *J Huazhong Univ Sci Technol Med Sci* 27:415-418.
- Zhao LR, Risedal A, Wojcik A, Hejzlar J, Johansson BB, Kokaia Z (2001) Enriched environment influences brain-derived neurotrophic factor levels in rat forebrain after focal stroke. *Neurosci Lett* 305:169-172.
- Zhao LR, Mattsson B, Johansson BB (2000) Environmental influence on brain-derived neurotrophic factor messenger RNA expression after middle cerebral artery occlusion in spontaneously hypertensive rats. *Neuroscience* 97:177-184.
- Zheng Y, Mao YR, Yuan TF, Xu DS, Cheng LM (2020) Multimodal treatment for spinal cord injury: a sword of neuroregeneration upon neuromodulation. *Neural Regen Res* 15:1437-1450.
- Zhou M, Wang H, Zeng X, Yin P, Zhu J, Chen W, Li X, Wang L, Wang L, Liu Y, Liu J, Zhang M, Qi J, Yu S, Afshin A, Gakidou E, Glenn S, Krish VS, Miller-Petrie MK, Mountjoy-Venning WC, et al. (2019) Mortality, morbidity, and risk factors in China and its provinces, 1990-2017: a systematic analysis for the Global Burden of Disease Study 2017. *Lancet* 394:1145-1158.
- Zou Q, Wu CW, Stein EA, Zang Y, Yang Y (2009) Static and dynamic characteristics of cerebral blood flow during the resting state. *Neuroimage* 48:515-524.

*C-Editor: Zhao M; S-Editors: Wang J, Li CH; L-Editors: Patel B, Haase R, Qiu Y, Song LP; T-Editor: Jia Y*

---